Comparison of Stator Winding Technologies for High-Speed Motors in Electric Propulsion Systems

T. Dimier, M. Cossale and T. Wellerdieck

***Abstract*—The stator winding is known to be a key factor to enhance the performance of electrical machines in terms of efficiency, lifetime, volume and consequently the costs. Therefore, the selection of the suitable winding technology and a proper design are mandatory to fulfill the challenging requirements defined by transportation electrification. The paper deals with the comparison of stator winding technologies to be used for high speed electrical machines for propulsion applications. The most commonly used winding configurations in automotive applications such as stranded wire and hairpin are compared with an innovative winding solution featuring formed litz wires. The analysis is carried out by comparing the main figures of merit such as the phase resistance, the AC loss factor and the thermal behavior of the different winding configurations. The reference machine explicitly designed for the analysis is a 24 krpm Permanent Magnet assisted Synchronous Reluctance Machine featuring a peak power of 200 kW. The performance assessment, supported by analytical and numerical electromagnetic and thermal simulations, highlights the main features of each design solution.**

***Index Terms*—vehicular propulsion, motor drives, electric motors, electric mobility, winding technology**

I. Introduction

Electric mobility is one of the major trends in the automotive industry aimed at reducing the greenhouse gas emissions [1]. The global electric fleet, consisting of battery electric vehicles (BEV) and plug in hybrid electric vehicles (PHEV), exceeded 5.1 million cars in 2018 and the number of sales has almost doubled with respect to 2017. One of the main goals for the development of electric vehicles is the reduction of cost and increase of mileage [2].

A key component of the electric vehicle is the drivetrain, comprised of the power electronic inverter, the motor and the gearbox [3]. Different motor topologies such as induction motors (IM), permanent magnet synchronous motors (PMSM), externally excited machines (EEM) are most commonly used in contemporary electric vehicles [4]. Increasing the power density of the electric motor for a given output power is one way to reduce the material cost of the electric motor. A prominent method to boost the power density for the PMSM is to increase the rotational speed of the machine for a given power rating resulting in a high-speed design [5], [6]. Another method is the enhancement of the cooling system, such as rotor cooling, spray cooling of the winding heads or cooling the stator slots directly. An additional possibility is to switch to winding technologies with an optimized fill-factor [7], such as hairpin windings (HPW). The latter usually also results in a reduction of manufacturing cost. However, combining the trend of the high-speed motor and HPW can lead to troubles due to the AC-losses, impacting the efficiency and the thermal management [8]. Therefore, loss mechanisms in the winding must be well understood if a high-speed design is developed.

This paper is focused on the PMSM since it provides a good compromise of power density and cost, even tough high-speed designs are also used for IMs and EEMs [9]. The most commonly used winding configurations in the automotive industry such as pull-in winding (PIW) and HPW are compared with an innovative winding solution featuring formed litz wires (FLW). The comparison is carried out using a reference, high-speed motor design.

The focus of the work presented in this paper is the comparison of different winding technologies. The modeling methods used by the authors are quoted from literature for the sake of brevity. More details can be found in the references.

This work was supported by EU H2020 project FITGEN (Grant Agreement 824335)

T. Dimier, M. Cossale and T. Wellerdieck are with BRUSA Elektronik AG, Neurdorf 14, 9466 Sennwald, Switzerland (e-mail: theophane.dimier@hpe.ee.ethz.ch).

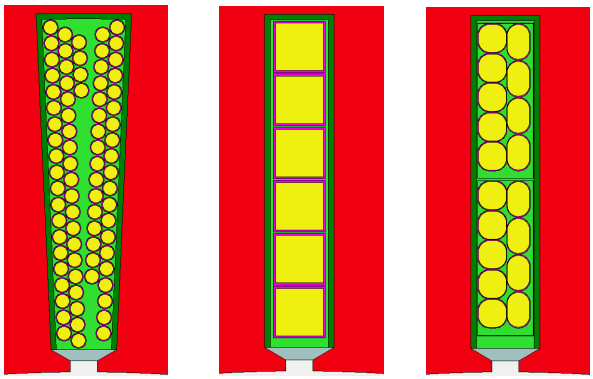

(a) (b) (c)

Fig. 1: Schematic view of one slot of the stator of the electric motor with pull-in winding (a), with hairpin winding (b) and with formed litz wire (c). Stator iron in red, conductor material in yellow and insulation in green (image created using Motor-CAD).

II. Winding technology

Distributed windings and slotted iron lamination stators are normally used for motors in traction applications. A schematic view showing the three different winding technologies discussed in this paper is shown in fig. 1. The winding technologies are described in section II-A, II-B and II-C.

A. Pull-In Winding

Pull-In Winding, also known as Stranded Winding or Random Winding, is shown in fig. 1a. It consists of round wires inserted into the slot. Each wire is insulated and multiple wires are connected in parallel. The position of each wire is not strictly defined but random since the windings are usually manufactured using flyer winding techniques for distributed windings. The winding head is manufactured using the winding material itself. Fill factors in the range of $40\ \%$ to $45\ \%$ are achieved for automotive applications. Usually, trapezoidal slots are used to maximize the winding area, c.f. section III-B.

The frequency dependent losses in PIW originate from three sources: skin-effect, proximity-effect and circulating currents. The first two effects can be controlled by selecting the appropriate strand diameter for the dominant electric frequencies while the latter is caused by the imbalance of induced voltage between parallel strands. Circulating currents have been found to be a major source of AC losses [10], [11]. To model each of these frequency dependent effects, the model described in [12] will be used in this study.

B. Hairpin Winding

Hairpin Winding, also known as Bar Winding is shown in fig. 1b. It consists of solid copper bars which are separately insulated. HPW is manufactured by inserting prefabricated, U-shaped bars into the slots of the machine. The open ends of the bars are then bent and connected by means of soldering or welding. The bending process defines the minimum dimensions of the bars which limits the amounts of bars per slot and, thus, the degrees of freedom of the winding design. The connection process is also the cause of asymmetric winding head dimensions of HPW machines. Fill factors exceeding $50\ \%$ are possible with HPW. The fill factor is reduced by the fact that the corners of the bars used for HPW are round due to the manufacturing of the bars. Additionally, a minimum clearance must be ensured between the bars for the assembly. These effects reduce the fill factor and are mainly significant for small bar dimensions.

The frequency dependent copper losses in HPW originate from skin and proximity effects. Proper connections of the bars within the machine avoid circulating currents between parallel turns. This constraint on the connections reduces the flexibility in the number of parallel and series turns [8]. The skin and proximity effect reduction for HPW is limited by the minimum bar dimensions defined by manufacturing process as mentioned above. The frequency dependent effects will be modelled in this study by using the method described in [13], modified to account for lateral insulation of the slot.

C. Formed Litz Winding

Formed Litz Winding, as shown in fig. 1c, consists of bars made by compressing twisted bundles of parallel connected strands. The technology is similar to Roebel bars. The individually insulated strands are continuously transposed along the axial direction of the motor [14]. The strand position is not random as in PIW but predefined. The axial transposition ensures a balanced thermal behavior of the FLW bar. A thin strand insulation is sufficient, since the voltage difference between parallel strands is small. The insulation to the stator or other phases is realized for the whole bar. The connection of the litz wire bars to form the winding pattern is realized using a proprietary technology by BRUSA which can not be disclosed. Two FLW conductors per slot are shown in fig. 1c. The fill factor achievable with FLW is comparable to HPW.

The frequency dependent losses in FLW originate from skin and proximity effects. The impact of these effects is reduced by selecting litz wire strands with small cross sections. Circulating currents within the bar should be minimal since the bar is electrically symmetrical due to its twisted nature. Even if small, the AC effects still exist and are modelled in this study using the model described in [15].

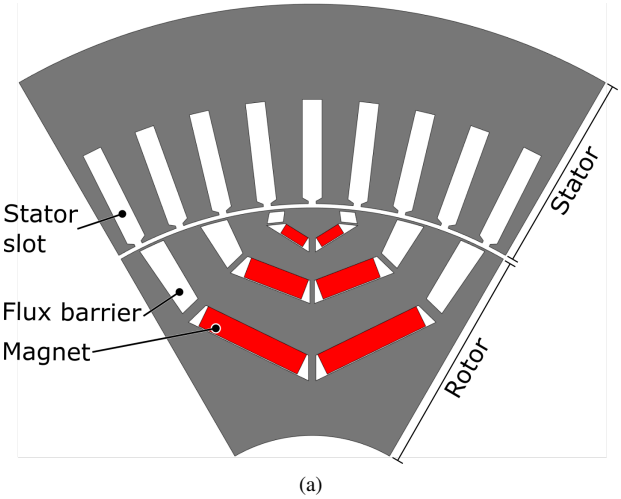

(a)

Fig. 2: Schematic view of one pole of a Permanent Magnet Synchronous Machine consisting of a rotor with buried permanent magnets and a stator (i.e. a permanent magnet assisted synchronous reluctance machine).

III. Reference Motor

A. Main Machine specifications

A six pole Permanent Magnet assisted Reluctance Machine (PMaRel, also known as Internal Permanent Magnet Machine or IPM) is used to compare the three winding technologies in a fair and consistent way. A high-speed design is used for reasons stated in section I. A schematic view of one pole is shown in fig. 2a. The peak power is of the machine is $200\,\mathrm{kW}$. Constant torque is available from stand-still to $10\,000\,\mathrm{rpm}$. For higher speeds the machine is operated in field weakening mode. The maximum speed is $24\,000\,\mathrm{rpm}$ which corresponds to an electric frequency of $1200\,\mathrm{Hz}$. The machine is water-cooled using a conventional cooling jacket in the stator housing and an encapsulation of the end-windings. The main specifications of the machine

TABLE I: Main specifications of the reference machine used for the comparison of the winding technologies.

Parameter	Value
Active length	179 mm
External stator diameter	176 mm
Number of pole pairs	3
Number of phases	3
Maximum speed	24 000 rpm
Maximum supply frequency	1200 Hz
Peak power	200 kW

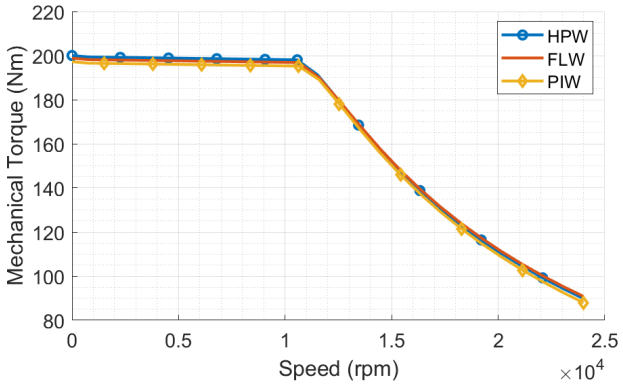

Fig. 3: Peak torque achievable with each design variant of the reference motor using PIW, HPW and FLW. The time at peak torque operation is limited due to thermal constraints.

are summarized in tab. I and the winding specifications are shown in tab. II.

B. Design variants

Three design variants are derived from the reference design to compare the three different winding technologies, PIW, HPW and FLW. The design variants exhibit similar magnetic behavior, c.f. fig. 3.

1) Pull-In Winding: Trapezoidal slots can be used for PIW, as discussed in section II-A. This allows for a wider slot area and, therefore, a larger copper area in the slot. However, there is a trade-off between slot area and width of the iron teeth. The trapezoidal slots are designed to have the same torque capabilities for a given current as the rectangular slots of the HPW and FLW design to ensure fairness of the study.

The winding is composed of six bundles of parallel strands per slot. The strands have a copper diameter of $0.6\,\mathrm{mm}$. The achieved fill factor is $42.2\,\%$ and the total copper area is $22.9\,\mathrm{mm}^2$. As explained above, the distribution of the strands within the slot is stochastic. Therefore, three case of strand placement have been considered:

- Best-case: parallel strands are spread along the width of the slot (tangential to the rotor surface).
- Worst-case: parallel strands are spread along the length of the slot (normal to the rotor surface).
- Intermediate case: the bundles of parallel strands are assumed to have the same shape factor as the slot.

TABLE II: Winding specifications of the design variations of the reference motor used for the comparison.

	PIW	HPW	FLW
Slot Area	$54.3\,\mathrm{mm}^2$	$44.4\,\mathrm{mm}^2$	$44.4\,\mathrm{mm}^2$
Copper area	$22.9\,\mathrm{mm}^2$	$23.9\,\mathrm{mm}^2$	$24.2\,\mathrm{mm}^2$
Fill factor	$42.2\,\%$	$52\,\%$	$52.7\,\%$
Strand size	$0.6\,\mathrm{mm}$	$2.1\times2.1\,\mathrm{mm}$	$1.29\,\mathrm{mm}$
End winding length	$80\,\mathrm{mm}$	$70.1\,\mathrm{mm}$	$48\,\mathrm{mm}$

2) Hairpin Winding: The design variant using HPW uses rectangular slots. The winding is a six-layer topology. Each bar has a cross section of $4\,\mathrm{mm}^2$. The achieved fill factor is $52\,\%$. The fill factor is impacted by the following effects:

- the narrow width of the slot and the small cross section of the conductor bars make the width of the insulation significant;
- the rounded edges of the bars due to manufacturing have a relevant impact.

3) Formed-Litz Winding: The third design variant uses FLW. Two FLW bars are stacked in per slot. Each bar is made of individual conductor strands with a diameter of $1.29\,\mathrm{mm}$ (AWG 16). The strands are twisted along the active length of the bar. This results in a magnetically and thermally balanced bar. The strands are insulated from each other and the whole bar is insulated, similar to the bars used for HPW.

C. Comparison of the three variants

PIW has a lower fill factor than HPW and FLW but the larger slot area reduces the difference of actual copper area per slot. The copper area of PIW is only $4.2\,\%$ and $5.4\,\%$ smaller than the HPW and FLW copper area, respectively. The axial length of the end winding is also considered. In this regard, FLW presents a clear advantage over the other technologies. This results in a more compact motor design. Furthermore, the winding head length has an impact on the resistance since longer axial length implies longer conductors. A schematic view of the machines showing the different winding head lengths is shown in fig. 4.

The phase resistances of the three windings are calculated for a temperature of $150\,^\circ\mathrm{C}$ over the electric frequency range exhibited during operation. The computation is performed using the models quoted in section II, implemented in MATLAB. The selected temperature is the maximum allowable for continuous operation. The results of the phase resistance calculation are shown in fig. 5. The resistance at selected operation points is presented in tab. III.

Several observations can be made regarding the results of the phase resistance calculation. The higher DC resistance of the PIW is a result of the longer end windings. The significant rise of the phase resistance at high frequency exhibited by the PIW, even for the best-case geometric arrangement, is due to circulating currents, c.f. section II-B. The DC resistance of the HPW and the FLW is essentially the same due to the similar copper area. The main difference arises at high

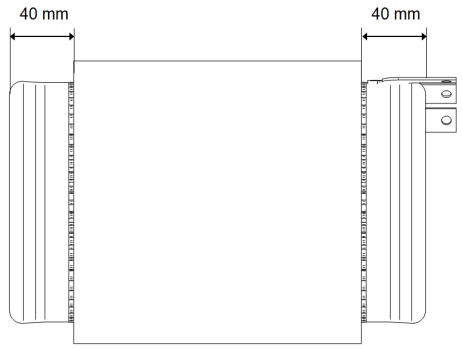

(a)

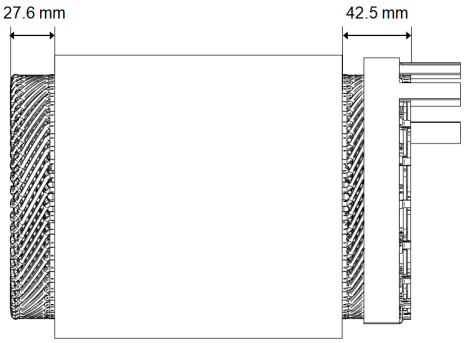

(b)

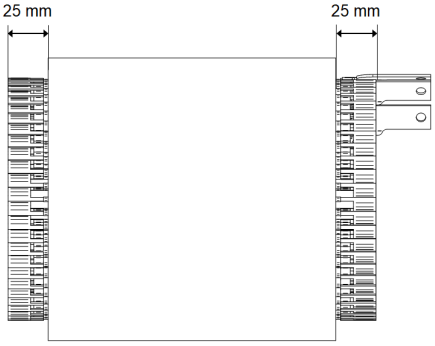

(c)

Fig. 4: Lateral view of the three design variants: PIW (a), HPW (b) and FLW (c).

TABLE III: Phase resistances of the PIW, HPW and FLW designs for selected operation points (150 °C). All values are normalized with respect to the DC resistance of FLW.

	Electric frequency		
Phase resistance (pu)	0 Hz	500 Hz	1500 Hz
PIW, intermediate	1.20	1.57	4.27
PIW, best-case	1.20	1.37	2.67
PIW, worst-case	1.20	2.01	6.33
HPW	1.06	1.17	2.04
FLW	1	1.01	1.07

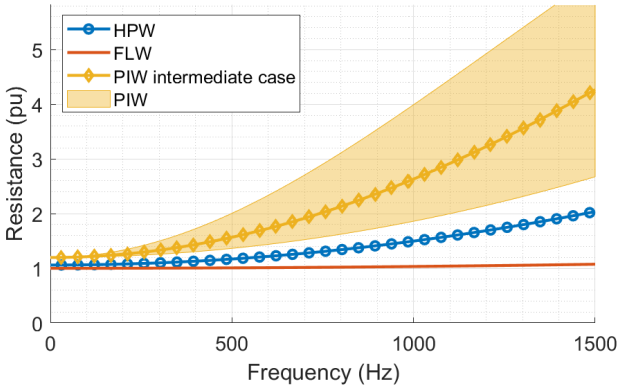

Fig. 5: Phase resistance of the PIW, HPW and FLW design over electric frequency for an operation temperature of 150 °C. All values are normalized with respect to the DC resistance of FLW.

electric frequencies where the magnetic balancing and the small cross section of the litz wires results in significantly lower AC resistance for FLW. The difference between the AC resistance of HPW and FLW is quadratic with respect to the electric frequency and is moderate at low speed. FLW and HPW have a phase resistance of 1.01 pu and 1.17 pu at 500 Hz, respectively. At high-speeds the difference is much more prominent with a phase resistance of 1.07 pu (FLW) and 2.04 pu (HPW) at 1500 Hz.

IV. Performance Assessment

A fair comparison of the winding technologies is only possible if the motor performance is analyzed. Comparing the performance allows to also cover thermal aspects of the windings. The design variants presented in section III-B have been analyzed in two ways:

- The efficiency and the losses are compared for a reference torque-speed profile.
- The maximum possible torque over speed is compared in isothermal operation, i.e. by finding the torque for each speed which results in a constant temperature of 150 °C at the winding hot spot.

The latter comparison results in the maximum continuous power for each speed. Below the two methods are described in detail.

A. Method

1) Reference profile: A reference torque-speed profile, displayed in fig. 6a, is considered to compare the three designs. The reference profile consists of two parts. For speeds from 0 rpm to 10 000 rpm the torque is at approximately 95.5 Nm. The mechanical power at the motor shaft is rising from 0 kW to 100 kW. The mechanical power is kept constant at 100 kW for speeds over 10 000 rpm. The losses and the motor efficiency were calculated using a combination of finite element (FEM) methods and analytical calculations for a motor temperature of 150 °C.

2) Isothermal operation: The maximum torque, and subsequent losses, are calculated over the speed range such that:

- the voltage and current constraints are obeyed;
- the temperature in the winding does not exceed $150\,°\mathrm{C}$ in steady state operation.

The procedure to establish the isothermal torque-speed profile for each design variant is:

1) A three-dimensional grid of operation points is defined. The dimensions of the grid are: the current amplitude, the load-angle and the motor speed.
2) The iron losses and the copper losses are calculated using FEM (ANSYS Maxwell) and analytical modelling, respectively. The losses are calculated for a machine temperature of $150\,°\mathrm{C}$. The iron losses are very sensitive with respect to current angle variations.
3) The steady state temperature is calculated for each operation point in the grid. The iron and copper losses are used as an input for the temperature calculation. Thermal networks in Motor-CAD are used for the temperature calculation.
4) The mechanical torque and power is calculated for each point in the grid.

The losses, the temperatures and the torque are now defined for each point in the three-dimensional grid. In a next step, the operation points are found which satisfy the isothermal condition:

5) A two-dimensional isosurface is extracted from the grid. The isosurface describes machine operation conditions in which the winding temperature is $150\,°\mathrm{C}$.
6) For each speed the operation point with the maximum torque is found on the isosurface.

This calculation method does not use any iterative loops since the temperature of the machine is defined a-priori, so it must be noted that the loss calculation is only correct on the isosurface.

B. Results

1) Reference profile: The results of the analysis using a reference torque-speed profile are displayed in fig. 6. Figure 6b shows the copper losses for the three design variants. The copper losses rise for speeds from $0\,\mathrm{rpm}$ to the edge speed of $10\,000\,\mathrm{rpm}$. The reduction in copper losses above the edge speed is due to the reduction of the torque in the field weakening range. This falling trend is more than compensated by the additional AC resistance of the PIW and the HPW winding. The copper losses of PIW and HPW are roughly three times and $62\,\%$ higher than the copper losses of FLW at $24\,000\,\mathrm{rpm}$. The iron losses, c.f. fig. 6c, are similar for the three machines since the torque is equal. These two effects result in reduced efficiencies for the PIW and the HPW design variant when compared to the FLW design as shown in fig. 6d. This shows the advantages of using FLW in high-speed machines since the efficiency has a direct impact on the required battery capacity for a given range requirement of the vehicle.

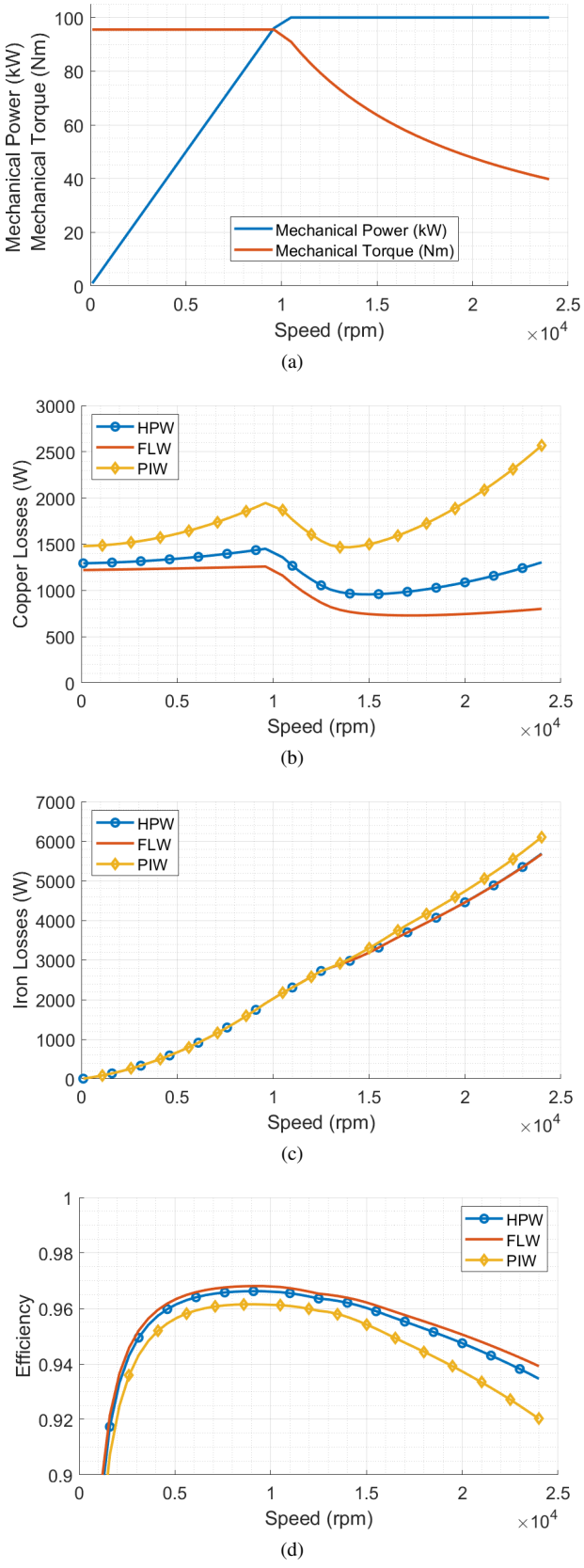

Fig. 6: Analysis of the three design variations of the reference machine showing the reference torque-speed profile and the mechanical power (a), the copper losses (b), the iron losses (c) and the efficiency (d).

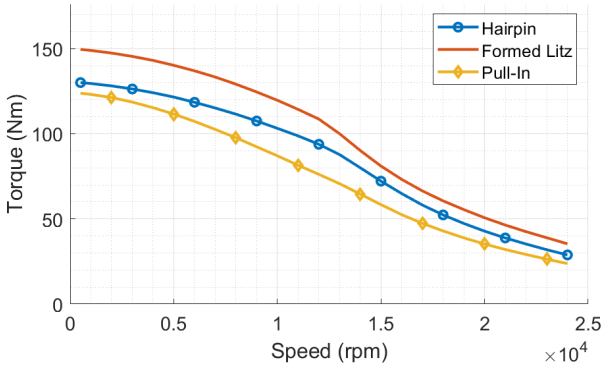

(a)

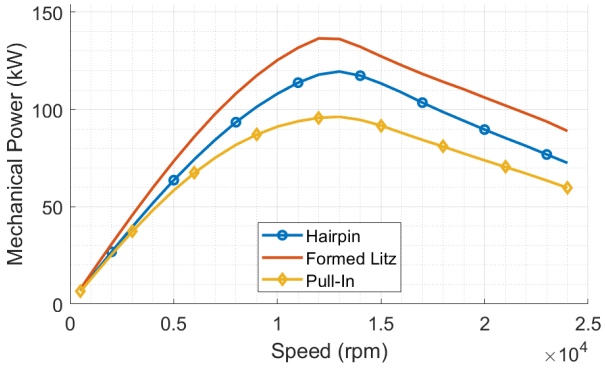

(b)

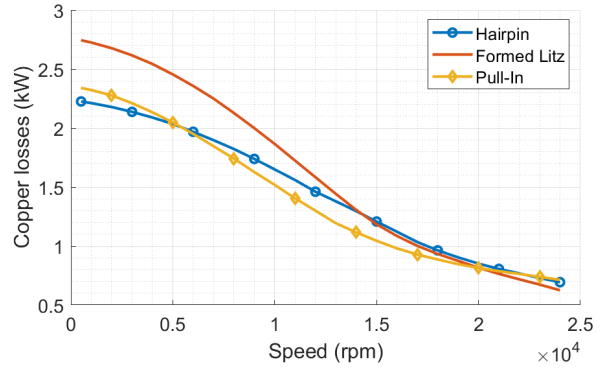

(c)

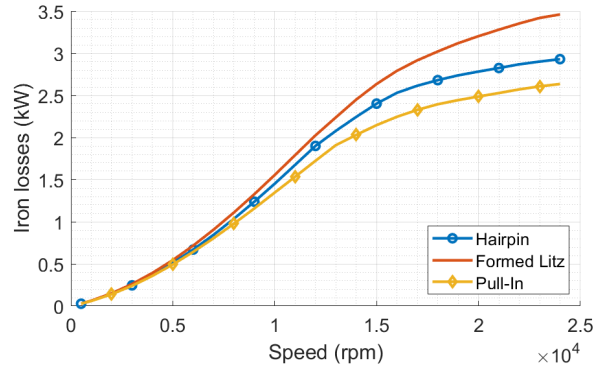

(d)

Fig. 7: Analysis of the three design variations of the reference design in isothermal operation at 150 °C showing the achievable torque (a), the mechanical power (b), the copper losses (c) and the iron losses (d).

TABLE IV: Key Performance indicators for the three design variants of the reference motor.

	PIW	HPW	FLW	unit
Box volume (housing included)	8.8	8.5	7.8	L
Motor speed: 0 rpm				
Continuous torque	124	130	150	N m
Continuous torque density	14.1	15.3	19.2	N m L^{-1}
Motor speed: 10 000 rpm				
Continuous power	91	108	125	kW
Continuous power density	10.3	12.7	16.0	kW L^{-1}
Efficiency at 100 kW	96.1	96.6	96.8	%
Motor speed: 24 000 rpm				
Continuous power	60	73	89	kW
Continuous power density	6.8	8.6	11.4	kW L^{-1}
Efficiency at 100 kW	92	93.5	93.9	%

2) Isothermal operation: The results of the isothermal operation are shown in fig. 7. The advantage of FLW with respect to the torque and power generation, fig. 7a and fig. 7b, are evident at all speeds. The maximum power at maximum speed is 89 kW for FLW, while it is only of 60 kW for PIW and 73 kW for HPW. Figure 7c shows that the copper losses of the three technologies are similar at maximum speed. This indicates that the smaller resistance of FLW allows for higher winding currents resulting in higher iron losses, c.f. fig. 7d. The improvement in torque and power is also due to the compactness of the end-windings since more compact winding heads result in a better copper to potting material ratio and, therefore, a better thermal behavior.

The improved thermal linking of the winding and the cooling jacket also results in increased performance at low speeds. The standstill torque reaches almost 150 N m for FLW but only 130 N m for HPW and 123 N m for PIW. The DC phase resistance is very similar for the three technologies, especially for HPW and FLW, therefore, the difference in torque can only be explained by the thermal behavior of the three technologies.

V. Discussion and Outlook

Key performance indicators are calculated at 0 rpm, 10 000 rpm and 24 000 rpm in order to compare the three design variants of the reference motor, c.f. tab. IV.

The first outcome of this study is the disadvantage of PIW for high-speed machines considering both continuous power density and efficiency. The technology exhibits higher copper losses and lower efficiency due to the higher phase resistance over the whole speed range. The losses are not only a drawback in terms of efficiency but also in form of the additional heat that must be removed in continuous operation. The thermal behavior of PIW further adds to the challenge to adequately cool the windings.

The DC phase resistance of HPW is improved with respect to PIW, but at high-speeds, the AC effects become significant, leading to high copper losses. Nevertheless, the good thermal properties of HPW reduces the impact of copper losses with respect to the total losses in the motor. This allows for a higher continuous power and a higher efficiency.

The study shows that FLW is well suited for high-speed applications with thin slots. The high fill factor, comparable to HPW, and the compact end windings are the cause of the low DC resistance. The continuous transposition of the wires enables a balancing of the magnetic flux over all the strands, unlike pull-in winding which then faces circulating currents amongst the strands. The twisting of the strands and the compact end windings also improves the thermal behavior. FLW allows for the highest continuous power densities and efficiencies.

The study shows that FLW is the technology with the highest KPIs among the chosen winding configurations. The performance of both HPW and FLW exceeds the performance of PIW.

VI. Conclusion

The two state of the art technologies for winding of electric motors for transportation applications have been compared with FLW to assess the advantages of each technology in terms of winding resistance, losses and efficiency over a reference profile and isothermal operation torque and power.

Considering the aspects analyzed in this study, PIW should be disregarded for high-speed motors, FLW is the highest performing technology for high-speed traction motors and HPW is a valuable alternative for machines operating at lower electric frequencies.

References

[1] S. Williamson, M. Lukic, and A. Emadi, "Comprehensive drive train efficiency analysis of hybrid electric and fuel cell vehicles based on motor-controller efficiency modeling," *IEEE Transactions on Power Electronics*, vol. 21, no. 3, pp. 730–740, May 2006.

[2] International Energy Agency (iae), "Global EV Outlook 2019," 2019.

[3] B. Frieske, M. Kloetzke, and F. Mauser, "Trends in vehicle concept and key technology development for hybrid and battery electric vehicles," in *2013 World Electric Vehicle Symposium and Exhibition (EVS27)*, Nov 2013, pp. 1–12.

[4] J. de Santiago, H. Bernhoff, B. Ekergård, S. Eriksson, S. Ferhatovic, R. Waters, and M. Leijon, "Electrical motor drivelines in commercial all-electric vehicles: A review," *IEEE Transactions on Vehicular Technology*, vol. 61, no. 2, pp. 475–484, Feb 2012.

[5] N. Bianchi, S. Bolognani, and F. Luise, "Potentials and limits of high-speed pm motors," *IEEE Transactions on Industry Applications*, vol. 40, no. 6, pp. 1570–1578, Nov 2004.

[6] N. Bernard, R. Missoum, L. Dang, N. Bekka, H. Ben Ahmed, and M. E. Zaïm, "Design methodology for high-speed permanent magnet synchronous machines," *IEEE Transactions on Energy Conversion*, vol. 31, no. 2, pp. 477–485, June 2016.

[7] H. Park and M. Lim, "Design of high power density and high efficiency wound-field synchronous motor for electric vehicle traction," *IEEE Access*, vol. 7, pp. 46 677–46 685, 2019.

[8] G. Berardi and N. Bianchi, "Design guideline of an ac hairpin winding," in *2018 XIII International Conference on Electrical Machines (ICEM)*, Sep. 2018, pp. 2444–2450.

[9] D. Fodorean, D. C. Popa, P. Minciunescu, C. Irimia, and L. Szabó, "Study of a high-speed motorization for electric vehicle based on pmsm, im and vrsm," in *2014 International Conference on Electrical Machines (ICEM)*, Sep. 2014, pp. 2577–2582.

[10] A. Lehikoinen, "Circulating and eddy current losses in random wound electrical machines," Ph.D. dissertation, Aalto University, Sep. 2017.

[11] M. van der Geest, H. Polinder, J. A. Ferreira, and D. Zeilstra, "Current sharing analysis of parallel strands in low-voltage high-speed machines," *IEEE Transactions on Industrial Electronics*, vol. 61, no. 6, pp. 3064–3070, June 2014.

[12] D. Bauer, P. Mamushkin, H.-C. Reuss, and E. Nolle, "Influence of parallel wire placement on the ac copper losses in electrical machines," in *IEEE International Electrical Machines & Drives Conference*, 2015.

[13] W. Zhang and T. M. Jahns, "Analytical 2-d slot model for predicting ac losses in bar-wound machine windings due to armature reaction," in *IEEE Transportation Electrification Conference and Expo*, Dearborn, MI, USA, 2014.

[14] H. Hämäläinen, J. Pyrhönen, J. Nerg, and J. Talvitie, "Ac resistance factor of litz-wire windings used in low-voltage high-power generators," *IEEE Transactions on Industrial Electronics*, vol. 61, no. 2, pp. 693–700, Feb 2014.

[15] C. R. Sullivan and R. Y. Zhang, "Simplified design method for litz wire," in *29th IEEE Applied Power Electronics Conference and Exposition*, Fort-Worth, TX, USA, Jan. 2014.

Théophane Dimier received his BSc. and MSc. from EPFL (Switzerland) in 2017 and 2019, respectively. He worked at BRUSA Elektronik AG as a Master thesis intern from February 2019 and as Motor Model Engineer from September 2019 to March 2020. Since March 2020, he is working towards a PhD. at the Laboratory for High Power Electronic Systems at ETH Zurich. His main research interests concern Power Magnetics and drives.

Marco Cossale received his M.Sc degree in Mechatronics Engineering and PhD in Electronics Engineering from Politecnico di Torino (Italy), in 2011 and 2017, respectively. From 2012 to 2016, he has been with Dipartimento Energia, Politecnico di Torino (Italy). During 2017, he worked as a research engineer with Johannes Kepler University, Linz, (Austria). Currently he is with BRUSA Elekronik AG (Switzerland) developing next generation of electrical drives for e-mobility. Dr. Cossale has co-authored more than 30 papers published in technical journals and conference proceedings. He serves as reviewer for some IEEE Transactions and international conferences. His main research interests concern design and thermal management of high-efficiency electrical machines.

Tobias Wellerdieck received his MSc. and PhD. in electrical engineering from ETH Zurich (Switzerland) in 2014 and 2018, respectively. From 2014 to 2018, worked with the Power Electronic Systems Laboratory, ETH Zurich (Switzerland). Currently he is with BRUSA Elektronik AG (Switzerland), responsible for system level simulations. His main research interest concerns control systems, power electronics and mechatronics for e-mobility applications.